Paper for 19th ICAS Conference
(18-23 September 1994, Anaheim California, USA)

PREDICTION & EVALUATION OF VECTORED JETS-INDUCED INTERFERENCE ON AIRCRAFT CONFIGURATIONS IN LOW-SPEED FLIGHT

Dr. R. K. Nangia

Consulting Engineer
Nangia Aero Research Associates
Maggs House,
78-Queens Road,
Bristol, BS8 1QX, UK

ABSTRACT

For V/STOL (or STOVL) aircraft, the prediction of vectored jet-induced effects during transition phase and manoeuvres is an important aspect in the understanding, design, control and operation of such aircraft.

This paper is concerned with a theoretical prediction method for multiple-jet-induced effects on STOVL aircraft during transition phase and out of ground effect. A semi-empirical modelling of the jet is used within the framework of subsonic singularity methods. Comparisons with experiments on a wing-body configuration have demonstrated acceptable agreement. Overall, the emphasis has been on predicting jet interference effects on practical configurations with multi-jets; forward and aft nozzles. Configuration related effects presented include: tails, which operate in a very much stronger jet downwash than the wing, strongly deflected slotted TE flaps, which can reduce jet interference, and under-wing stores.

This procedure can enable optimisation studies to be undertaken prior to experimental programmes. The design cycle can be commenced with a good idea of configuration restraints, relative effectiveness of the various controls, and the changes needed in the flight control system to cope with partially jet-borne phases of flight. There is a significant potential for encouraging cost and time savings.

Avenues for future work and improvements of the model have been proposed. These aspects will contribute to current and future practical STOVL developments.

1. INTRODUCTION

For V/STOL or STOVL aircraft, the prediction of vectored jet-induced effects during the transition phase and manoeuvres is an important aspect in the understanding, design, control and operation of such aircraft. Transition from jet borne to wing borne flight may occur In Ground Effect (IGE) or Out of Ground Effect (OGE). Currently many different types of layouts are being studied, Fig.1 (Refs.1-8). Some of these are developments of the "four-poster" Harrier concept whilst others (two- or three- posters with and without canards), are aimed at multi-role missions with supersonic capability.

Vectored thrust implies effects that are "direct" (resolved thrust force and moments) and "indirect" (induced on surfaces, controls or intakes). The "indirect" effects are often adverse. Future ASTOVL aircraft may have exhaust nozzles a long way from the CG making balancing much more critical. This in turn means operating within relatively tight aerodynamic and powerplant configuration limits during the approach phase. Therefore, for design of control systems with adequate safety margin, a large database with parametric variations of the aircraft geometry variables and the jet parameters is required. Trim and balance studies need to allow for the forces at the empannage in strong jet downwash. Forces arising on stores are also needed.

Because of the evident need to proceed mainly on an experimental basis and the high cost and time factors implicit in wind tunnel tests or full-scale trials, progress on this subject, to date, has been relatively slow. The experiments have ranged from exploring fundamental jet flows with and without wind tunnel constraint (Refs.9-22) to more configuration related aspects. Several review papers have been published (e.g. Refs.23-26). The current project scene although more "paced" emphasises cost and time reductions.

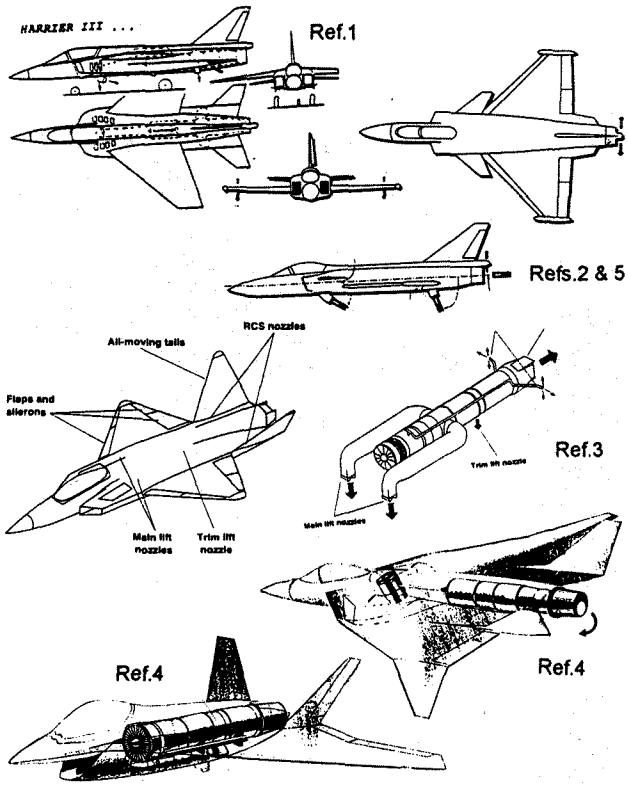

FIG. 1 TYPICAL JET-INTERFERENCE V/STOL & STOVL CONFIGURATIONS OF DIFFERENT LAYOUTS

Several workers have described the features of a jet deforming in a cross-flow, the entrainment and the formation of counter-rotating vortices downstream (Fig.2). On neighbouring surfaces, two effects are likely. The first is to produce an aerodynamic image of the jet. The second exists mainly for the jet in close proximity to, or on the surface and causes viscid interactions upstream and downstream of the jet. The high velocities in the initial region of the jet and the associated entrainment effects are not well understood at present. Interpretations are different from various authors.

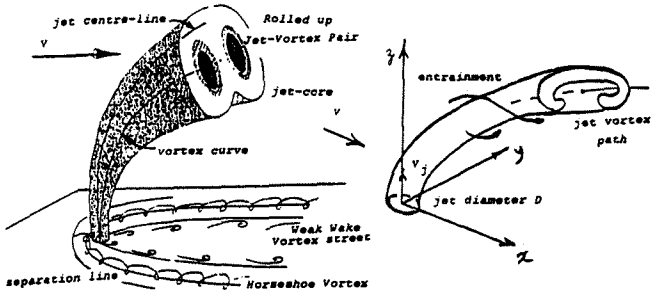

FIG. 2 SKETCH OF JET IN CROSS-FLOW & SEMI-EMPIRICAL MODEL

The detailed CFD formulations (Navier-Stokes) of vectored-jets are not yet sufficiently mature to become tools for routine design and analysis. One recent example is by Chiu et al (Ref.27) from a thin layer Navier-Stokes calculation for a 90° circular jet in cross-flow. The solutions were found to be sensitive to the far-field boundary conditions and the radial grid clustering near the edge of the jet. After some 20,000 iterations, convergence had not been obtained in local detail. Use of a fine clustered grid in the region upstream of the jet exit allowed the horseshoe vortex in the boundary layer near the jet exit to be captured. More importantly for aircraft applications, some of the computed plate pressure distributions compared favourably with the experiment of Fearn and Weston (Refs.13-16) over most of the surface.

Practical Applications & Topics Covered

In the context of practical project applications, an "effective" way (in time, cost, flexibility and confidence) has been to build a semi-empirical jet model. This model has been incorporated within the framework of subsonic singularity methods. The technique enables prediction of multiple-jet-induced effects on aircraft during the transition phase and out of ground effects.

This paper outlines the features and physical arguments of the predictive technique and presents comparisons with existing experiments conducted on a wing-body configuration. It then leads on to predictive results of practical interest.

2. THEORETICAL CONSIDERATIONS OF SEMI-EMPIRICAL JET MODEL

The theoretical considerations leading to development of the semi-empirical model of the jet have been presented in Refs.9 and 10. The basic proposition is that the cross-flow momentum is transferred to a streamwise vorticity in a gradual manner, releasing the volume of air as an expiration. The strength of the jet is modelled with doublet and source/sink distributions. The vortex path is described empirically.

This model, based on a re-examination of data on the jet plume (Jordinson, Ref.11, Fearn and Weston, Refs.13-16), has led to a formulation of a semi-empirical jet model depicted in Fig.2. This takes into account the work of Keating (unpublished, RAE, 1989), Bradbury (Ref.18), Smy (Ref.19), Wooler (Ref.20), Hackett (Ref.21), Ashill & Keating (Ref.22) and others (Refs.12, 17, 20). Generally, experience indicates that the model is valid for geometries where the neighbouring surfaces are about one jet diameter away from the nozzle. This does not preclude considering cases where the neighbouring surfaces are closer because the effects are localised near the nozzle and convenient limits on induced velocities can be introduced if required.

For a jet issuing from a surface, local viscid interactions are present upstream and downstream of the jet. These interactions do not need to be included for application to "practical" flowfields where the jet nozzle is displaced from the wing (or the fuselage) surface and therefore jet near-field effects can be minimised. This does not however imply inclusion of the local blunt-body flows around the nozzle and body intersections.

A line doublet located along the vortex-line of the jet gives a circular displacement surface with stagnation lines similar to those found in experimental data (Fearn and Weston, Refs.13-16) as shown in Fig.3. The model therefore implies the imaging effect of the flat plate. However, in relation to the approximations involved in setting up the basic jet model, the imaging effect is relatively small.

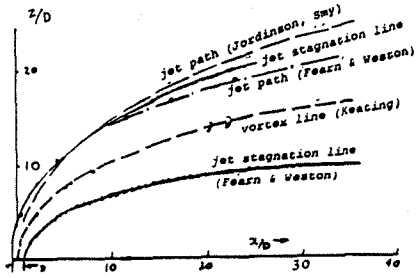

FIG. 3 COMPARISONS OF JET PATHS, R = 8, Θ_{j0} = 90° (BASED ON WORK BY KEATING)

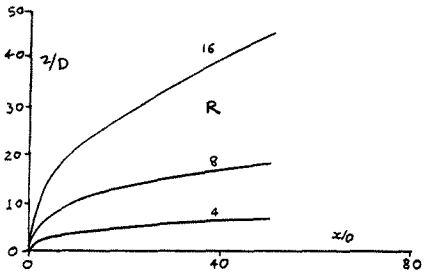

FIG. 4 JET VORTEX PATHS FOR DIFFERENT VALUES OF R, Θ_{j0} = 90°

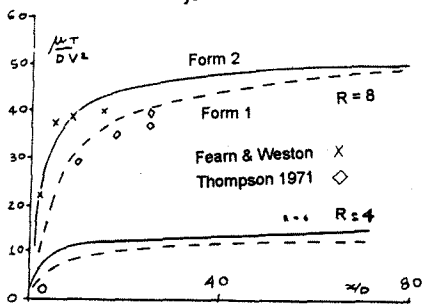

FIG. 5 DOUBLET STRENGTH OF JET Θ_{j0} = 90°, R = 4 & 8

Fig.4 shows the jet vortex paths generalised from Fig.3 for different jet velocity ratios R = V_j/V issuing normally, Θ_{j0} = 90°. The cosh formula of Jordinson is adapted for simplicity, as explained in Ref.9, with a single multiplying constant. Along the jet vortex path, are placed: doublets for lifting effects and momentum changes, sources to represent the volume displacement of the injected mass flow, and sinks to represent the jet plume.

Fig.5 shows the doublet strength for R = 4 and 8 compared with experimental results from papers by Fearn and Weston (Refs.13-16) and Thompson (Ref.12). This also emphasises the different results obtained from experimental measurements.

For the jet issuing at Θ_{j0} < 90°, the jet path can be derived with the aid of a virtual jet origin (Θ_{j0} = 90°) displaced forward from the real jet origin (Θ_{j0} < 90°). This procedure has been followed for the R = 8 jet.

Fig.6 illustrates the effect of varying jet deflection angle Θ_{j0} on the streamwise variations of jet parameters: height z/D, doublet strength μ_T and source strength σ_v. The source term σ_v depends strongly on the variation of Θ_j with respect to s. Consequently this term decreases sharply with decreasing jet deflection angle Θ_{j0}. The term is appreciable for jet deflection angles Θ_{j0} between 75° to 90° but very small for Θ_{j0} < 75°. The σ_{v0} term is also small for relatively small jet nozzles and for Θ_{j0} near 60°.

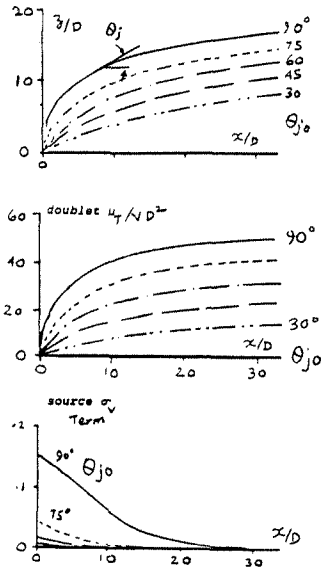

FIG. 6 EFFECT OF Θ_{j0} VARIATION ON JET PARAMETERS IN NEAR-FIELD, R = 8

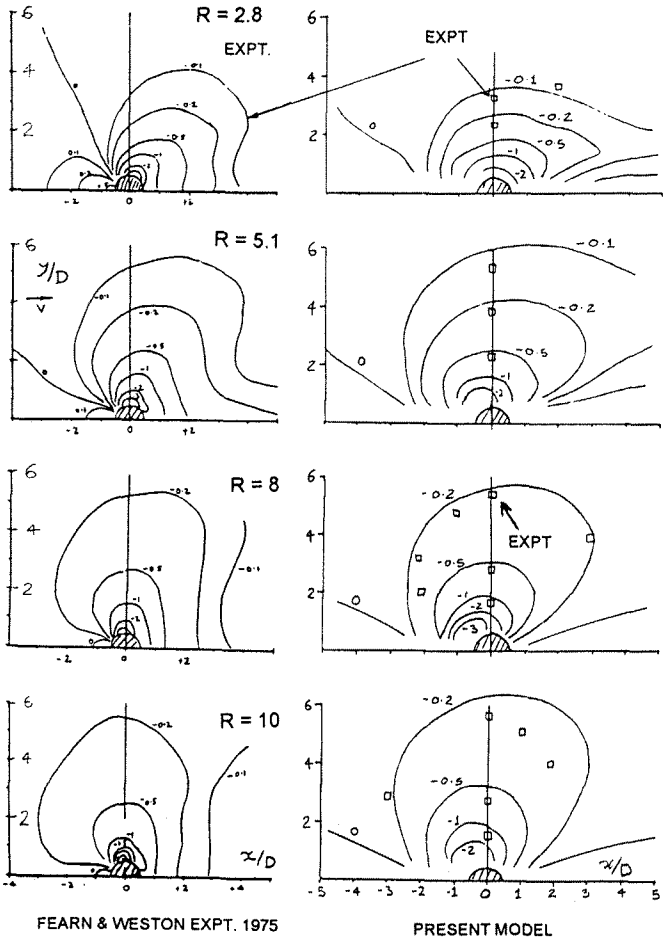

FIG. 7 COMPARISONS OF C_p CONTOURS ON A FLAT PLATE DUE TO JET, R VARIES

The velocity induced at a general point in space due to doublet and source distributions along the jet can be written following the potential flow equations derived in a standard text such as Ref.28. The estimates can be used in a conceptually simple validation case of pressures induced on a flat plate.

Pressures Induced by a Jet Issuing from a Flat Plate

Assuming that the vertical velocity induced by the jet is cancelled by its image in the flat plate, total C_p follows by doubling up the expression for C_p from the non-dimensional velocity components u and v calculated for one jet as:

$$\text{Total } C_p \text{ (2 Jets)} = 2\, C_p \text{ (1 jet)} = 2\,(-2u - u^2 - v^2).$$

Fig.7 shows C_p contours induced on a flat plate due to a jet issuing normally (Θ_{j0} = 90°). The results from the present doublet jet model have been compared against Fearn's experiment (Refs.13-16). The recent measurements of Ref.29 agree closely with Fearn's data. Note that this comparison is really an extreme case and a rather critical check of the theoretical model since estimates are for the effects due to a jet which is not displaced from the surface and high induced velocities are implied (C_p near -4.0 at the edge of the nozzle). Further, wake effects of the jet on the flat plate surface are also present.

Over the forward region of the plate, where jet and surface boundary layer interaction can be considered minimal, there is, overall, a fair to good agreement between the theory and experiment. The agreement is emphasised for low R values as the contours are relatively "asymmetric" about the spanwise axis. At higher R, the contours tend towards "symmetry" about the spanwise axis as the jet vertical extent increases. The predictions are once again acceptable for large R and away from the jet and surface boundary layer interaction zones.

The favourable comparisons both, on jet stagnation lines (Fig.3), and the induced C_p comparisons have given confidence to pursuing further work. If necessary, in future, improved correlations between theory and experiment for given R may be obtained by varying one of the empirical factors. In the current work, the emphasis is on "practical" flows where the jet nozzle is usually displaced from the neighbouring surfaces.

3. THE JET MODEL INCORPORATION IN SURFACE SINGULARITY METHODS

For wing-body modelling, several choices with aerodynamic singularities are possible. These range from simple vortex lattice adaptations to complex higher-order panel methods. In the first instance it is prudent and desirable to keep the modelling aspects simple and concentrate on the jet interference effects for symmetric flow situations.

3.1. Lifting Surface (Wing-body) Approach

As in panel methods, surface source elements are used to model a circular cross-section body (without boat-tailing), Fig.8. The flow "displacement" effect of the body at zero incidence is easily handled in this way.

The jet in close proximity to the fuselage implies potentially large normal and tangential velocities over the fuselage control points. With the surface sources on the body only, this would require a large concentration of "strong" panels near the jet. A form of internal (fuselage) singularity distribution is required that will enable cancellation of the majority of the large normal induced velocities. A general and reasonably elegant technique is to introduce a series of 3-D point sources (or sinks) placed inside the fuselage (0.3 to 0.6 times local radius r) at a number of cross-sections in the vicinity of the jet, just to image the jet plus fuselage. The number of 3-D sources per cross-section equals the number of control points at each cross-section and the strengths of these sources follow from collocation of normal velocities at the body surface.

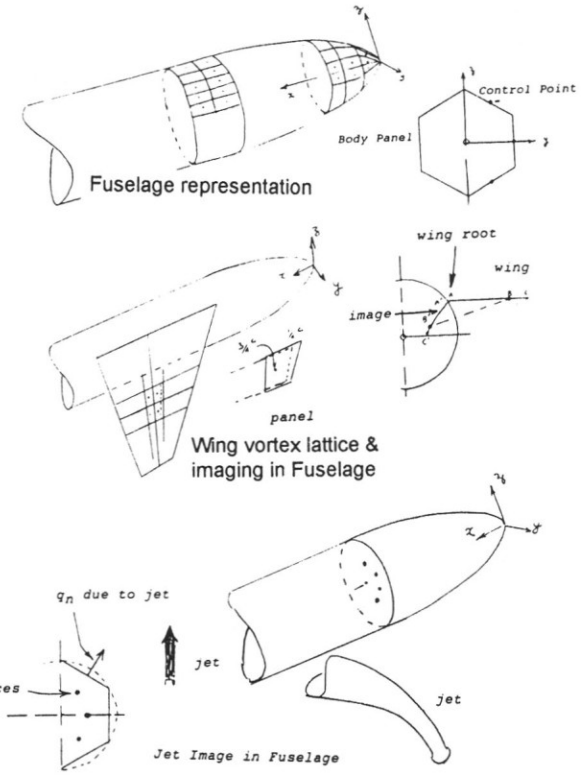

FIG. 8 FEATURES OF THEORETICAL MODELLING

This procedure has the advantage that the flow incidence effects on the body can be included along with the jet effects; the surface panels remain "weak", dealing only with residuals, enabling use of fast, efficient algorithms.

Based on Ref.30, the wing is modelled as a thin lifting surface (vortex-lattice with imaging inside the fuselage). With this technique, the normal velocity body condition is approximately satisfied. The body source panels and internal sources provide the remaining "correction terms".

In terms of panelling efficiency and hence computer usage, the adopted procedure offers a very significant step forward towards a practical application. It allows a complete "de-coupling" of the jet effects from the wing-body problem and a modular approach can be set up. This transpires because the jet is relatively insensitive to local variations in velocity whereas the wing and body are sensitive to the jet function.

The solution to the overall problem follows from the boundary condition of zero normal velocity at control points over the fuselage and the wing. An influence coefficient approach is adopted to determine the unknown body source panel strengths and the wing vorticity. Pressures and loadings are determined after calculating the surface tangential velocities. The wing trailing wake can be relaxed, although this is not considered to be first-order significant.

3.2. More General Developments

The above approach can be adapted to improve the modelling of the fuselage geometry. For example, non-circular or elliptic sections can be derived using conformal transformation techniques. The aft parallel body assumption allows the wing image trailing vortices to proceed without intersecting the fuselage. This limitation can be removed, if required, by curving the image trailing vortices. The effect of this will be small in most practical cases.

Wing thickness effects can be handled as in most panel methods with definition of upper and lower surfaces and this of course implies increased panelling. Similarly panel methods for complex fuselage shapes can be used.

At this stage, the twin-jet model is regarded as non-interacting, this being approximate, will require further detailed experimental information.

Extension to asymmetric cases can be visualised; both halves of the configuration will need to be included instead of invoking symmetry on one half.

4. EXPERIMENTS TO OBTAIN RESULTS FOR VALIDATION OF THEORY

The half-model VSTOL configuration tests in the DRA 13 x 9 ft low speed closed section Wind Tunnel (Fig.9) have provided a suitable example for validation of the theory.

4.1. Experimental Model

The half-model was mounted on an underfloor balance, the jet nozzle being connected to "earth" (turntable), so that forces registered were those due to the basic aerodynamics and jet-lift interference only, the forces on the nozzle external structure being ignored. Overall this approach has been considered more convenient and less expensive than two other alternatives, (i) reliance on extensive pressure measurements over the wing which then require accurate integration, and (ii) building a model incorporating a "live jet" that is likely to pose problems of accurate balance measurements and calibration of jet thrust.

The boat-tailed fuselage of "oval" cross-section has a slightly drooped nose. The body width y/s (at the wing TE) is 0.182. The "mildly" cambered and twisted wing, mounted "mid-high" on the body, has a thickness/chord ratio 8.5%, aspect ratio 3.4, taper ratio 0.325 and a leading edge sweep of 40°. Fourteen Pressure measurement stations on the wing are denoted by A to H, J to N and P. The stations A to M are closely spaced over the inner and middle wing to highlight the blown effects. The nozzle is located at y/s = 0.2467. There are no pressure measurement stations over the fuselage.

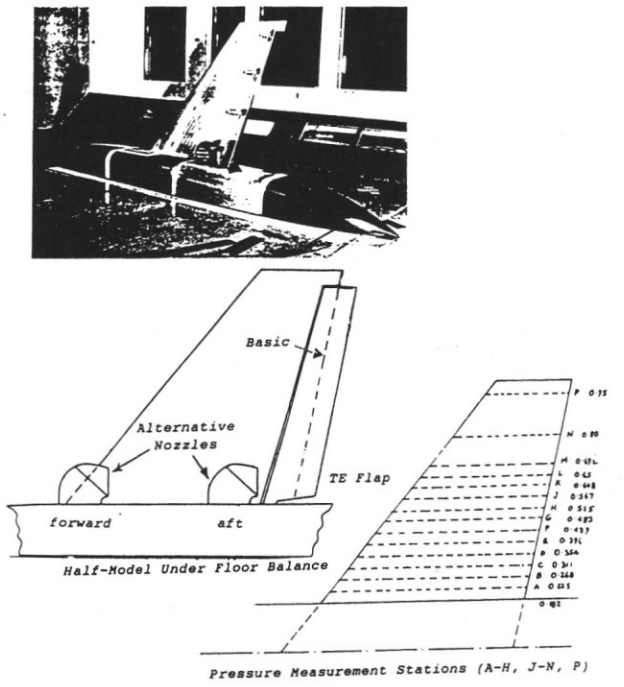

FIG. 9 VIEW OF TEST MODEL (WITH TE FLAPS) IN WIND TUNNEL & GENERAL FEATURES

Tests on the model have included: thrust variation (coefficient C_μ), different nozzles (nominally "large" and "small") and blowing geometry (nozzle position and deflection angle can be preset). It should be mentioned that the large jet nozzle is less than one diameter away from the fuselage and due to very close proximity, locally high induced velocities may arise. This can cause local separations initially which can trigger stronger separations over the body and the wing. Pressure measurements over the fuselage would be required to further the understanding of these aspects. In this paper, results refer to the large nozzle.

4.2. Forward Nozzle at 60° Deflection

The effect of jet blowing (C_μ = 0 and 0.448) on C_p distributions at various spanwise stations on the wing upper and lower surfaces at α = 0° is illustrated in Fig.10. The jet interference on the wing upper and lower surfaces is judged from the differential pressures (ΔC_{pj}). The local lift (ΔC_{LLj}) distributions have been derived from ΔC_{pj} distributions. To highlight the effect of the jet near-field wing pressures, Fig.11 compares the chordwise pressures at two wing stations A and B lying either side of the nozzle. Note that jet interference causes considerable re-distribution of the pressures with the strongest effects appearing near the jet nozzle (wing lower surface). The loss of lift and LE suction occurs over the whole wing.

4.3. Aft Nozzle at 60° Deflection

The effect of jet blowing (C_μ = 0 and 0.448) on C_p distributions at various spanwise stations on the wing upper and lower surfaces at α = 0° is shown in Fig.12. The jet interference on the wing upper and lower surfaces is indicated by the differential pressures (ΔC_{pj}) and the local lift (ΔC_{LLj}) distributions. Fig.13 compares the chordwise pressures at stations A and B lying either side of the nozzle. As in the previous case, the jet interference causes considerable re-distribution of the pressures with the strongest effects appearing near the jet nozzle. The loss in lift extends as far as 70% semi-span. The LE suction increases over the whole LE. Interference lift is positive all along the LE.

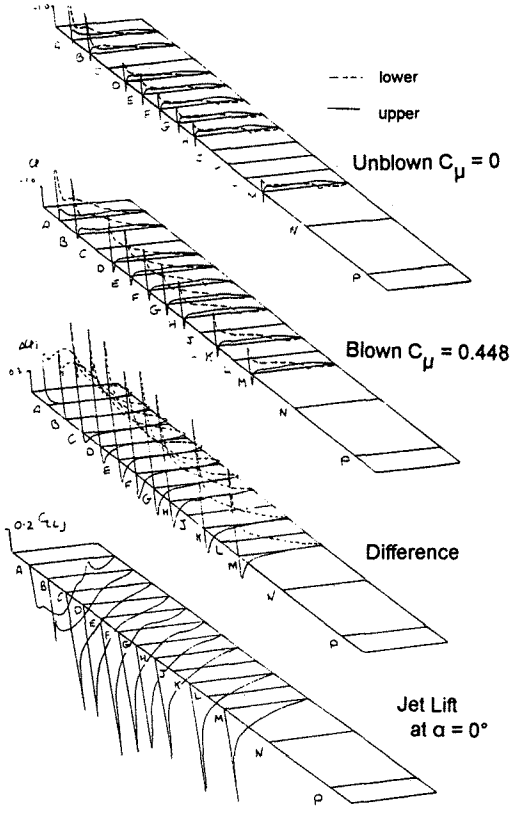

FIG. 10 C_p (C_μ = 0 & 0.448), ΔC_{pj}, C_{LLj} DISTRIBUTIONS, FORWARD NOZZLE, α = 0°, Θ_{j0}=60°

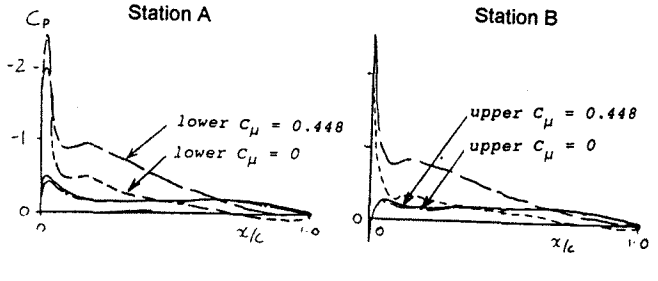

FIG. 11 C_p DISTRIBUTIONS AT STNS A & B, FORWARD NOZZLE, α = 0°, C_μ = 0 & 0.448, Θ_{j0}=60°

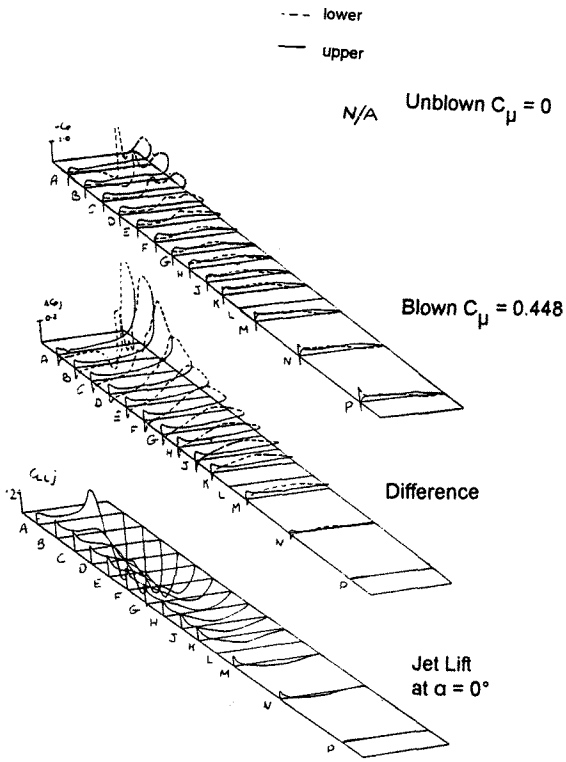

FIG. 12 C_p (C_μ = 0 & 0.448), ΔC_{pj}, C_{LLj} DISTRIBUTIONS, AFT NOZZLE, α = 0°, Θ_{j0}=60°

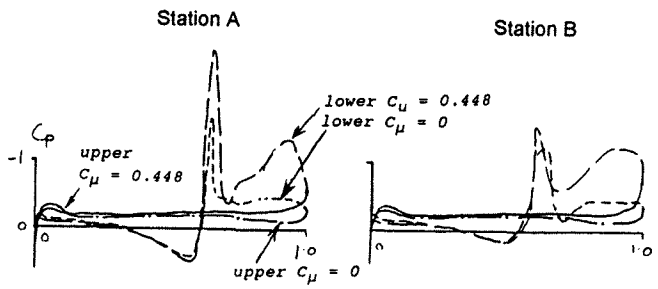

FIG. 13 C_p DISTRIBUTIONS AT STNS A & B, AFT NOZZLE, α = 0°, C_μ = 0 & 0.448 Θ_{j0}=60°

Figs.11 and 13 stress that the wing pressures at stations A and B for the unblown case are affected strongly by the presence of the nozzle and the associated blunt-body flows. Although the respective shapes are very different, an essential feature is that high suctions are caused due to blunt-body flows. Pressures on the wing without nozzles *in situ* were not available.

5. PREDICTED RESULTS & COMPARISONS WITH EXPERIMENT

5.1. Body + Wing, Theoretical Modelling

At this stage, the main intention is to derive the jet interference loading over the wing to visualise the strong effects present. Simple panel representations in keeping with the theory have been used intentionally as shown in Fig.14, e.g.

- An uncambered (flat-plate) wing (semi-span s) is set at zero incidence on a symmetric circular body at the -45° ("mid-high") location over the fuselage. The xyz axes system is placed with respect to the fuselage nose at (0,0,0). The measurement z_w denotes the vertical distance measured from the wing plane in the jet direction. The exposed wing panelling is 9 chordwise panels at 10 spanwise stations. The jet direction notation is kept positive upwards.

- The panelling is 24x8 stations over the fuselage which has y/s=0.16. Slight reduction in diameter compensates, to some extent, for the boat-tailing as well as getting nearer to keeping the minimum distance of the nozzle about one diameter away from the surface.

Fig.14 shows also the geometry details for the "large" jet nozzle (assuming Θ_{jo} set at 60°) in forward (near station 10) or aft (near station 15-16) locations. A small concern is that jet nozzle is less than one diameter away from the fuselage for both locations (Sections 2 and 3).

5.2. Body + Wing, Forward Nozzle at 60° Deflection

Fig.15 shows the vertical velocity induced due to the jet, inner body sources and the resulting chordwise loadings at 10 spanwise stations over the exposed wing.

The contribution due to the fuselage approximately "mirrors" the jet-wing contribution and the magnitude amounts to about a third of the effect due to the jets over the wing.

There is indication of a broad "concentration" of interference load over the inner wing. The interference, although reducing away from the nozzle, is still very significant all along the LE. This confirms the trends measured in experiment (Figs.10-11).

Fig.16 shows the spanwise loading $C_{LL}c/c_{av}$ compared with the experimental loading which has been derived from pressures integration of the data of Fig.10 (Section 4). Gross wing calculations are shown for reference. The theory under-predicts the experiment. In total force terms, see Fig.19, the agreement is however acceptable. This tends to indicate that a re-distribution of loads had occurred due to presence of the fuselage. Partly, this is due to the nozzle being located very near the wing root LE which causes blunt body flow. This may degrade the whole swept-back wing flow. A detailed experiment with pressure measurements on the fuselage would be required to illuminate this aspect.

5.3. Body + Wing, Aft Nozzle at 60° Deflection

Fig.17 shows the vertical velocity induced due to the jet, inner body sources and the resulting chordwise loadings at 10 spanwise stations over the exposed wing. The effects are favourable near the LE of the wing.

As for the previous case, the contribution due to the fuselage approximately "mirrors" the jet-wing contribution and the magnitude amounts to about a third of the effect due to the jets over the wing.

Fig.18 shows the spanwise loading $C_{LL}c/c_{av}$ compared with the experimental loading which has been derived from pressures integration of the data of Fig.12 (Section 4). Gross wing calculations are shown for reference. The theory predicts the experiment acceptably. In total force terms, see Fig.19, the agreement is also acceptable.

5.4. Comparison of Total Forces

Several parametric studies have been undertaken for comparison with experiment. One such study is presented here, briefly, to indicate the validity and potential. For simplicity, calculations were for wing only configurations. Fig.19 shows the effect of varying jet velocity (R = Vj/V) on a wing for the two nozzle positions (forward and aft). Lift loss is predicted for both nozzle locations. Comparisons with experiment show very encouraging correlation. The pressure measurement cases discussed in Section 4 are included on this figure (R = 4.585).

6. PREDICTIVE RESULTS OF PRACTICAL INTEREST

Results for cases of practical interest can now be presented although experimental results for validation are not available.

6.1. Combined Operation of Forward & Aft Nozzles

In practice, we need to know the effects of jet interference due to the combined operation of forward and aft nozzles. On VSTOL aircraft, design and balance considerations imply substantial differences in thrust levels of the forward and aft nozzles. In the present studies, we have assumed that the forward and aft nozzles operate at the same thrust and that the geometry parameters are the same as previously.

Fig.20 shows the chordwise loadings along the span. As might be expected, there are two peaks corresponding to the forward and aft nozzles. Fig.21 shows the spanwise loading compared with the cases for the forward and aft nozzles blowing separately. The interference for all nozzles operating is the sum of the constituent forward and aft nozzles contributions.

6.2. Simple Wing + Body + Tail Configurations

Figs.22 and 23 refer to a wing+body+tail configuration The wing is in "mid-high" location (as in Fig.14) on the fuselage, whilst the tail is in "mid-low" position. The jet nozzles can be forward or aft. The panel density has been kept low intentionally, to emphasise the main features. Fig.22 gives the chordwise interference loadings. Fig.23 shows the jet-interference spanwise loadings on the wing and tail. Note the extremely strong effects felt at the tail location (near to 10°-12° "wash" angle). The forward nozzle induces stronger effects on the wing while the aft nozzle causes stronger effects on the tail.

The practical implication is that tailplane deflection is likely to be very large to balance the interference loads due to vectored jets. Calculations with all jets operating need to be done. Indications are that to a first approximation, the interference loads arising are additive. This emphasises the need for careful positioning of jets in a given configuration (possibly splaying).

The results given here demonstrate the ability to provide an understanding of the large jet-induced effects on tails and also the ability to offer predictions for realistic geometry.

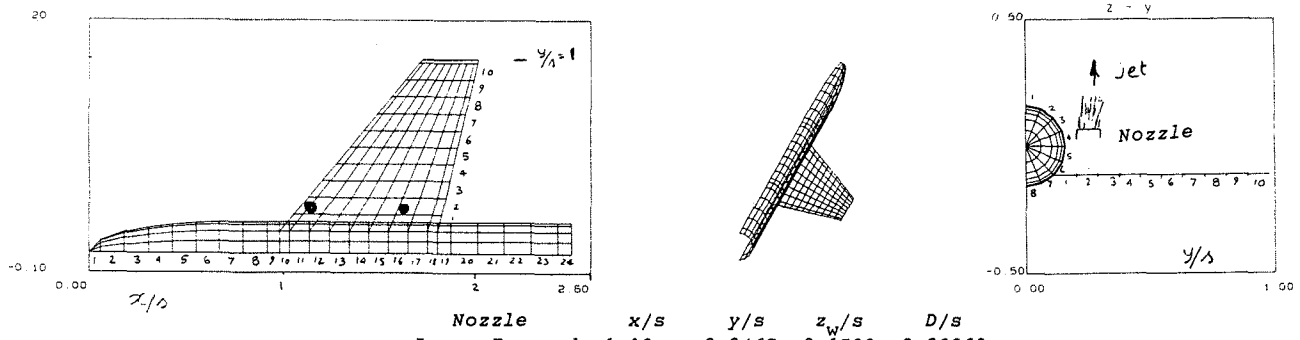

Nozzle	x/s	y/s	z_w/s	D/s
Large Forward	1.12	0.2467	0.1733	0.08963
Large Aft	1.6237	0.2467	0.1688	0.08963

FIG. 14 THEORETICAL MODEL FUSELAGE + WING & JET NOZZLE DETAILS

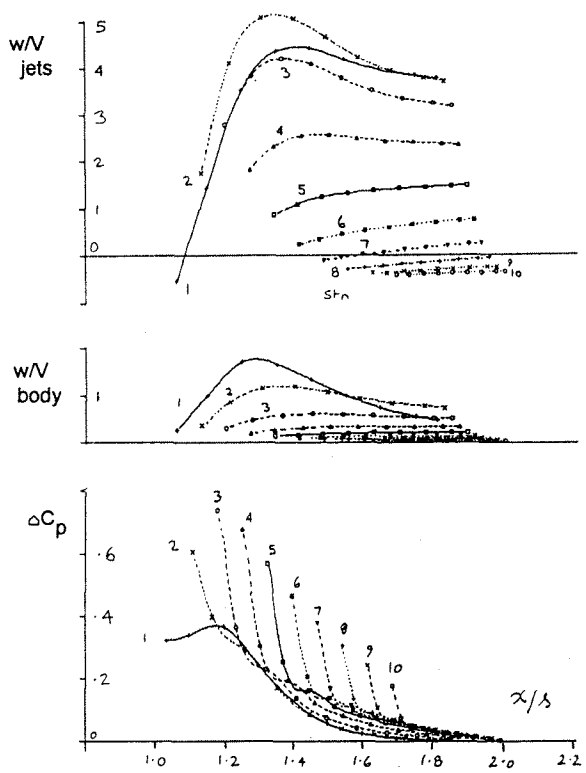

FIG. 15 w/V DUE TO JETS, BODY SOURCES & CHORDWISE LOADINGS ON WING, FORWARD NOZZLE
R = 4.585, C_μ = 0.448, Θ_{j0} = 60°

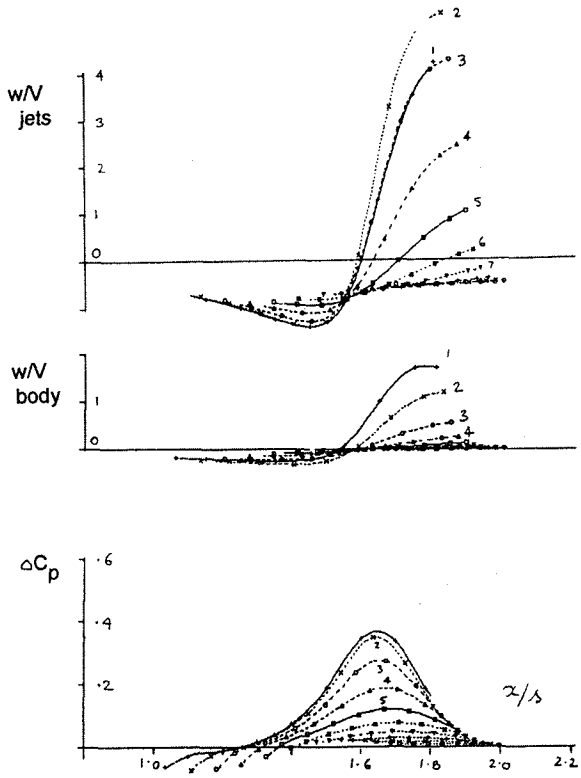

FIG. 17 w/V DUE TO JETS, BODY SOURCES & CHORDWISE LOADINGS ON WING, AFT NOZZLE
R = 4.585, C_μ = 0.448, Θ_{j0} = 60°

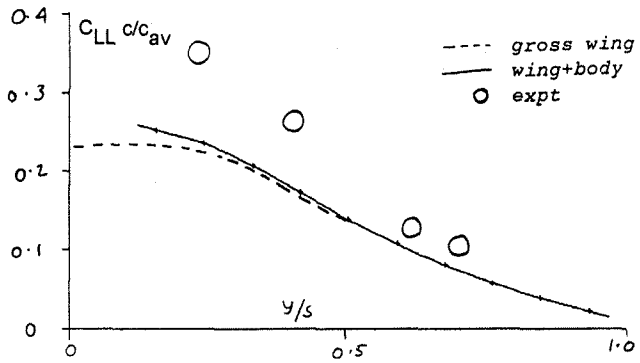

FIG. 16 JET INTERFERENCE $C_{LL}.c/c_{av}$ DISTRIBUTION, FORWARD NOZZLE, THEORY & EXPERIMENT,
R = 4.585, C_μ = 0.448, Θ_{j0}=60°

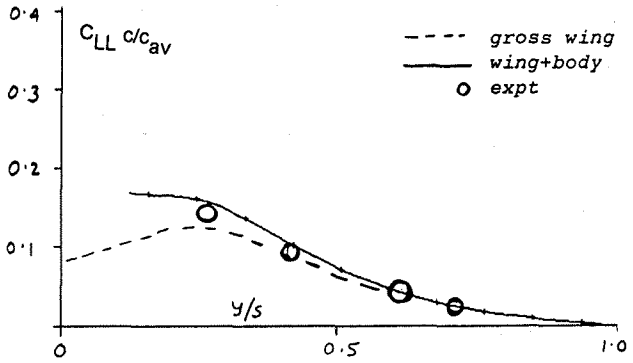

FIG. 18 JET INTERFERENCE $C_{LL}.c/c_{av}$ DISTRIBUTION, AFT NOZZLE, THEORY & EXPERIMENT,
R = 4.585, C_μ = 0.448, Θ_{j0}=60°

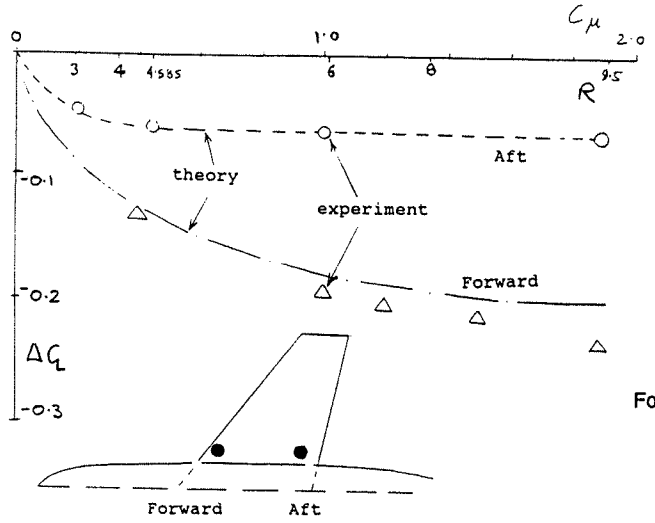

FIG. 19 LIFT LOSS DUE TO FORWARD or AFT JETS FROM NOZZLES, $\Theta_{j0} = 60°$, R & C_μ VARY

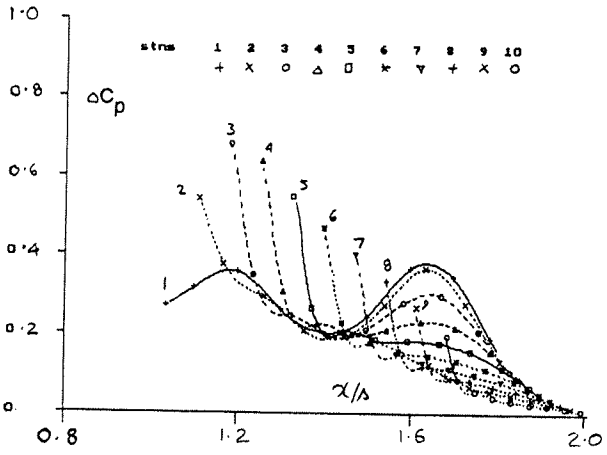

FIG. 20 WING OF (WING + BODY), JET-INDUCED CHORDWISE LOADINGS ALONG SPAN, FORWARD & AFT NOZZLES
R = 4.585, C_μ = 0.448, $\Theta_{j0} = 60°$

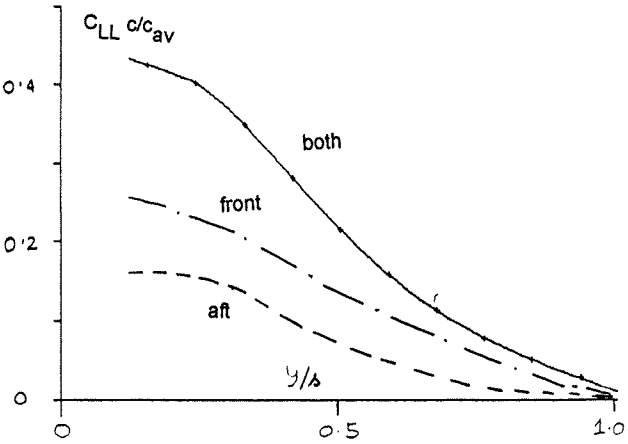

FIG. 21 WING OF (WING + BODY), JET INTERFERENCE C_{LL}·c/c_{av} DISTBn, FORWARD & AFT NOZZLES, y/s = 0.2467
R = 4.585, C_μ = 0.448, $\Theta_{j0} = 60°$

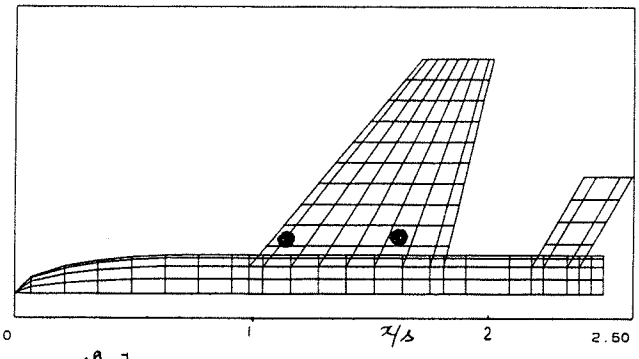

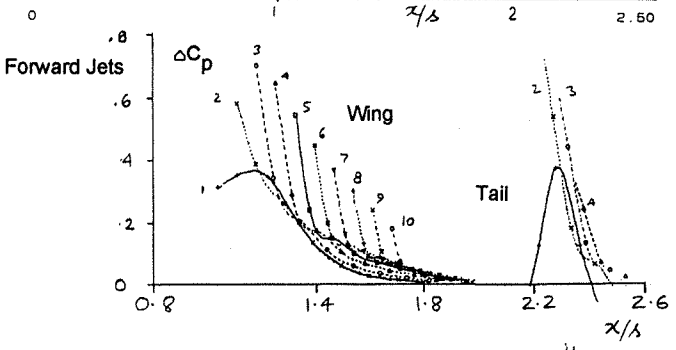

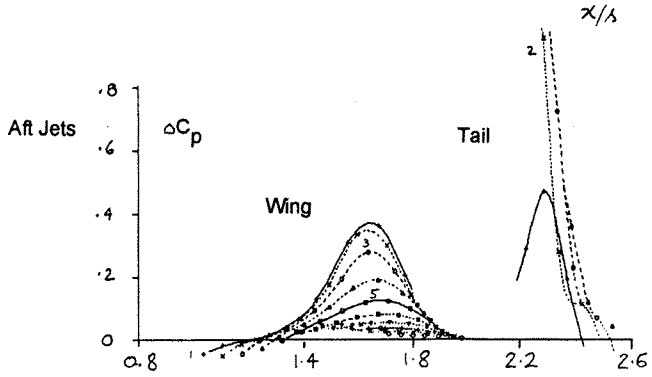

FIG. 22 JET-INDUCED INTERFERENCE ON A WING+BODY+TAIL CONFIGURATION, CHORDWISE LOADINGS
R = 4.585, C_μ = 0.448, $\Theta_{j0} = 60°$

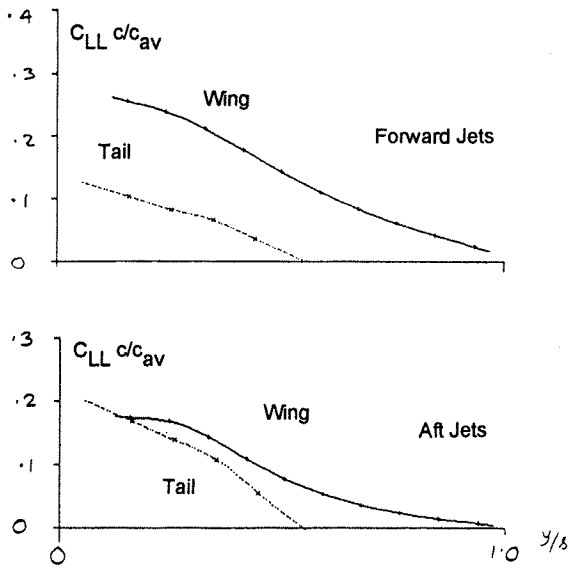

FIG. 23 JET-INDUCED INTERFERENCE ON A WING+BODY+TAIL CONFIGURATION, SPANWISE LOADINGS
R = 4.585, C_μ = 0.448, $\Theta_{j0} = 60°$

6.3. Studies with Thick Wings

A series of jet effects studies have been undertaken for a symmetric section, thick swept wing of aspect ratio 4.2. The jet direction is downwards for this case and the wing is at α=0°.

Fig.24 shows the effect of forward and aft nozzles, operating separately or together on chordwise pressures induced. Note that the forward nozzles operate at R = 5 whilst the aft nozzles operate at R = 7. Spanwise variations of normal and axial force and pitching moment due to jet interference are given in Fig.25. Note from Fig.24 that jet interference affects mainly the wing lower surface. This also confirms the trends observed in Figs.10 and 11 (Section 4). Fig.25 suggests that for this particular jets configuration, the lift loss is greater due to the aft jets but the pitching moment arising is mainly due to the forward jets.

Fig. 26 illustrates the effect for jet vectoring between 30°, 60° and 90° for an aft nozzle location on the same wing. The geometry parameters are different from the previous case. Spanwise variations of normal and axial force and pitching moment due to jet interference are depicted. Interference forces and moments increase as jet deflection increases. It follows from Figs.25 and 26 that drag forces can be predicted.

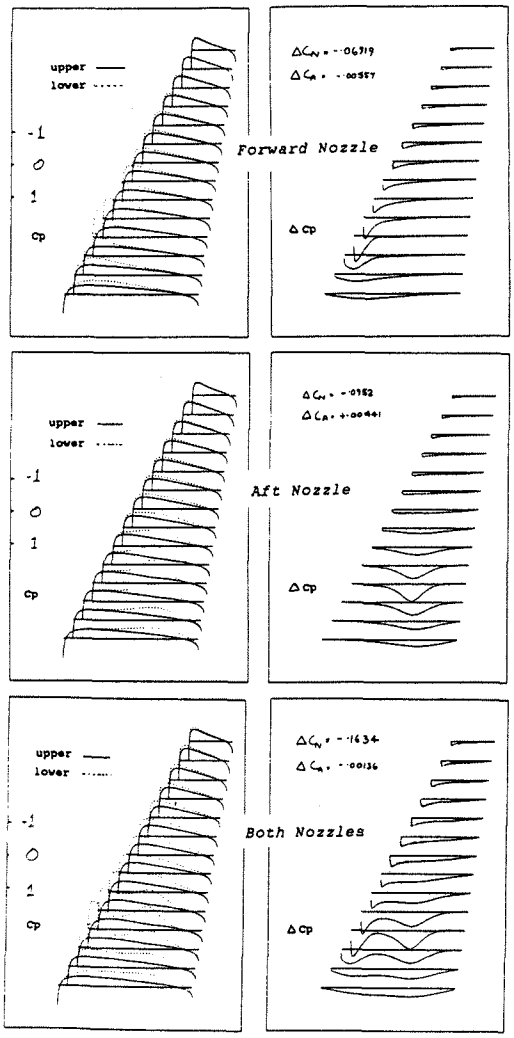

Nozzle	x/s	y/s	z/s	D/s	R
Forward	0.16	0.25	0.1	0.065	5
Aft	0.60	0.25	0.1	0.065	7

FIG. 24 THICK WING, FORWARD & AFT JETS OPERATING SEPARATELY OR TOGETHER, CHORDWISE PRESSURES INDUCED

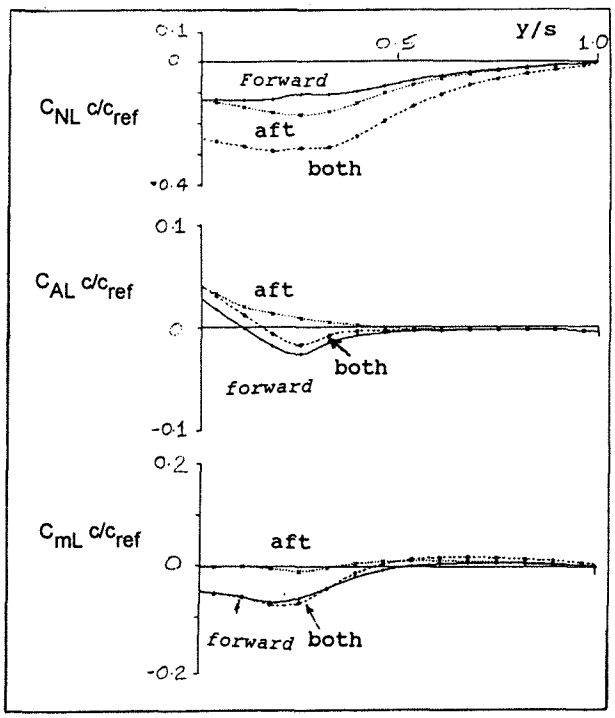

FIG. 25 THICK WING, FORWARD & AFT JETS OPERATING SEPARATELY OR TOGETHER, SPANWISE VARIATIONS OF NORMAL FORCE, AXIAL FORCE & PITCHING MOMENT

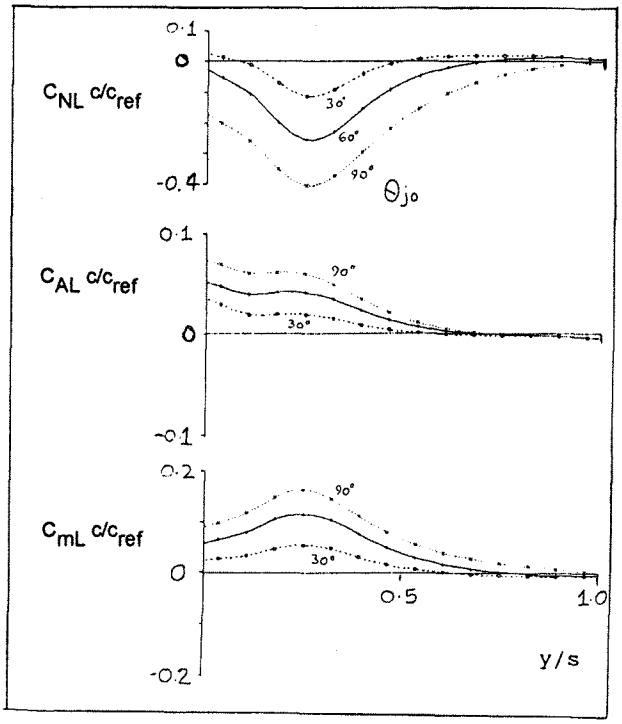

Nozzle	x/s	y/s	z/s	D/s	R
Aft	0.65	0.25	0.1	0.1	5

FIG. 26 THICK WING, THE EFFECT OF JET VECTORING ON SPANWISE VARIATIONS OF NORMAL FORCE, AXIAL FORCE & PITCHING MOMENT

6.4. Wing + Body with Slotted TE Flap

In STOVL aircraft, the jets are usually in close proximity to slotted TE flaps. To improve performance and manoeuvring, large flap deflections are scheduled with high jet deflections.

Here we present one example of a simplified high-wing and body configuration, based on a VSTOL arrangement (Ref.31) with a slotted TE flap. Fig.27 shows the jet interference loads due to forward and aft jets with deflection varying and operating at R = 8. Note the beneficial effect due to flap deflection particularly for the aft nozzle. Similar conclusions were drawn by Kuhn (Ref.24).

The benefits to be gained from optimising flap size and deflection and nozzle deflection are obvious. Further detailed modelling of this aspect is desirable, involving more realistic geometry, relaxed wakes and allowing for possible flow separations.

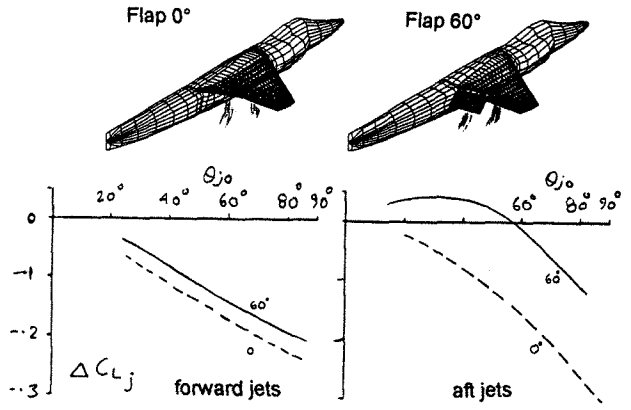

FIG. 27 EFFECT OF SLOTTED TE FLAP DEFLECTION ON LIFT DUE TO FORWARD & AFT JETS, R=8, Θ_{j0} VARIES

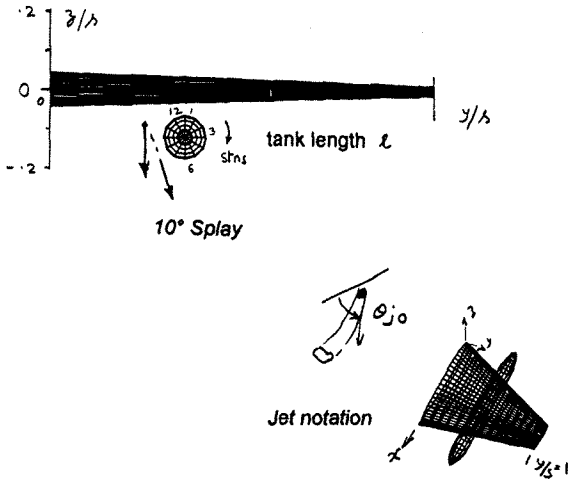

FIG. 28 WING & STORE CONFIGURATION FOR PRELIMINARY CALCULATIONS, Forward & Aft Nozzles

6.5. Jets & External Stores

STOVL aircraft usually carry external stores or tanks which are under very strong influence of the jets. For satisfactory installations, the interest is in:

- Store/Jet interactions to minimise lift loss, IGE or OGE
- Store loads and release and the influence of reacting jets
- Drag arising from incipient local separations or general pressure drag
- Influence of Store/Jet interactions on overall forces and control requirements

All these aspects can be addressed using the predictive method to obtained pressure distributions over the stores. Preliminary calculations on a wing-only case demonstrate the feasibility and also give a qualitative feel.

Fig.28 shows an aspect ratio 4 swept-wing (semi-span s) with a store (or a tank) located underneath. Pylons have been omitted for simplicity at this stage. The store has 12 chordwise generators (stations). Jets can be located forward or aft:

x/s=0.16 (forward) and x/s=0.5 (aft)
y/s=0.25, z/s=-0.1 measured from the wing apex at (0,0,0).
Forward Jet velocity ratio, R=5,
Aft Jet R=7, Splay angle 0° and 10°
Jet Deflection angle 60° (forward or aft jets)

Fig.29 shows the Cp distributions on the tank (along 12 generators) with either forward or aft jet blowing. The effect of splaying the aft jet by 10° is also shown. The results show the high -Cp values arising due to the jets proximity. Splaying jets increases the -Cp.

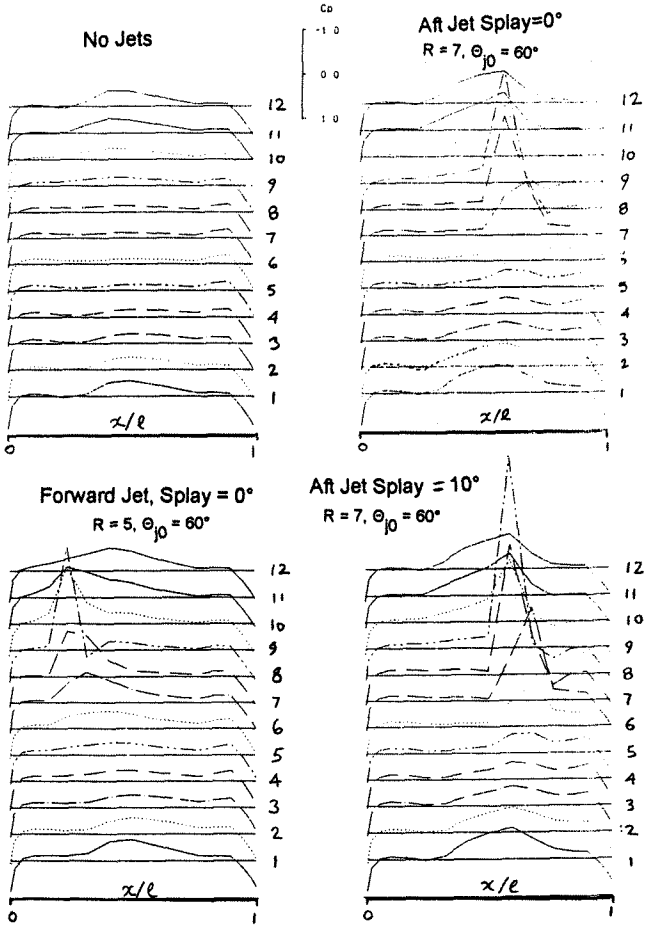

FIG. 29 Cp DISTRIBUTIONS ALONG 12 STORE GENERATORS, EFFECT OF FORWARD & AFT JETS, SPLAY ANGLE 0° & 10°

This confirms that the forces and moments arising are strongly dependent on store geometry and its placement relative to the jet. The forces on the store will tend to increase as the store size reduces. This aspect of work can enable investigation of several geometric variables to determine "safe" store locations. This capability, once verified, will have obvious benefits of very appreciable cost savings.

7. FURTHER WORK

Further verifications of the model are planned with more general controls and flaps. The results for realistic configurations with thick wings highlight the ability to undertake very useful parametric studies for practical aircraft. Optimisation studies can be carried out prior to experimental programmes. This process therefore has a very significant potential for providing cost and time savings.

The approach has also highlighted several major gaps in knowledge, indicating therefore the directions of research. Some areas for further work include the following topics.

- **Jet Modelling, Interacting 2, 3 or 4 jets.** The shape of one jet alters due to the presence of another jet nearby either in tandem or side-by-side. Improved knowledge base will lead to a better and more general jet model.

- **Systematic parametric studies of practical STOVL configurations (Fig.1) at small and large α.** This will allow the design cycle to commence with a good idea of the relative effectiveness of the various controls and the changes needed in the flight control system to cope with partially jet-borne phases of flight.

- **Effect of Wind Tunnel Interference on Jet flows.** For large strength jets, not impinging on the tunnel walls, there is a significant tunnel interference effect, not only in overall terms but also in variations along the span of the model. The wind tunnel jet interference needs therefore to be included in the calculations right from the start when making comparisons with experimental data.

- **Jet Effects on Lateral & Directional Characteristics.** Sideslip displaces the jet system laterally (Ref.24). The pressure distribution is shifted towards the downstream side of the configuration generating a jet-induced rolling moment. The rolling moment due to sideslip can be doubled by jet effects. This points towards the possible use of differential jet deflections for control. It is open to conjecture that the combination of the inlet-induced directional instability at low speeds plus the large jet-induced rolling moment due to sideslip may have been responsible for the loss of several jet V/STOL aircraft. It is therefore important to determine limiting conditions to optimise control power demands.

- **Control Jet Effectiveness.** The problems created by the jet induced rolling moments can be aggravated by the jet-interference on the effectiveness of the wing-tip roll-control jets. Such control aspects need investigation by extending the current approach.

- **Supersonic Jets.** The investigation of supersonic jets in subsonic cross-flow is a particularly difficult problem in a wind tunnel. The jet, having a large velocity ratio is likely to be strongly affected by the wind tunnel constraint.

- **Ground Constraint, High Jet Strengths.** When the jets strike the ground, rolled-up vortex sheets form at ground level which need to be introduced into the model. Jet/Ground interactions and Hot Gas Re-circulation (HGR) present a complex challenge for future analyses.

Work on these topics should have a constructive and practical impact on current and future programmes for STOVL aircraft. The pure CFD methods, although promising for future, are not sufficiently mature to become tools for active design. The implicit costs for extensive, in depth experimental studies are also prohibitive.

8. CONCLUDING REMARKS

The prediction of vectored jet-induced effects on V/STOL configurations during transition phase and manoeuvres constitutes an important aspect in the understanding, design, control and operation of such aircraft.

Vectored thrust implies "direct" (resolved thrust force and moments) and "indirect" (induced on aerodynamic surfaces / controls or intakes) effects. The "indirect" effects are often adverse. Satisfactory control of such aircraft, with sufficient margin for safety, requires therefore access to a large database with parametric variations not only of the aircraft geometry but also of the jet parameters.

The detailed vectored-jet models using field (Navier-Stokes) formulations have not reached sufficient maturity to become tools for active design and analysis. This has emphasised the need for "effective" alternative methods (in time, cost and flexibility).

In this paper, a semi-empirical modelling of the jet is used within the framework of subsonic singularity methods, for predicting jet interference effects on practical configurations with non-interacting (at present) multi-jet effects; forward and aft nozzles.

Modelling in the vicinity of the fuselage required particular care (high local induced velocities). An imaging technique with sources has facilitated the solution.

Comparisons with experiment have indicated good agreement with predictions for aft nozzle cases both in forces and pressures. For the forward jet nozzle in close proximity to the wing LE, the predicted forces were in good agreement but the pressures were under-predicted. Therefore, there is a need for improvement in technique and understanding. Further detailed experimentation would also be required.

From the point of view of trim and control of thrust-vectoring configurations, estimates for tail loads can be given. The tail is in a very much stronger jet downwash than the wing.

Jet interference studies for thick swept wings and wing+body configurations with TE flaps and under-wing stores have demonstrated the ability to obtain estimates of forces and moments.

Optimisation studies can be carried out prior to experimental programmes. This process will allow the design cycle to commence with a good idea of the relative effectiveness of the various controls and the features needed in the flight control system to cope with partially jet-borne phases of flight. Therefore there is a significant potential for encouraging cost and time savings.

Areas for further work and improvements of the model have been proposed. It is believed that these aspects will have a constructive impact on the current and future practical VSTOL and ASTOVL scene.

ACKNOWLEDGEMENTS

The author has pleasure in acknowledging helpful technical discussions with Mr. J.Hodges, the late (sadly) Mr. R.F.A.Keating, Dr. P.R.Ashill, Dr. B.R.Williams, Mr. P.M.Murdin, Mr. J. Peto and Mr. P.G.Martin at the DRA (UK). Technical comment by Mr. S.F.Stapleton on the paper is appreciated.

Part of the early work was supported by Aerodynamics & Propulsion Department of the DRA, Bedford UK.

Lastly it should be mentioned that any opinions expressed are the author's own.

REFERENCES

1. SEVERAL SPEAKERS, "Towards Harrier III", RAeS Conference, See Report by J.M.RAMSDEN, RAeS, Aerospace, Feb.1991.

2. HARRIS, A.E., WILDE, G.L. , SMITH, V.J., MUNDELL, A.R.G. & DAVIDSON, D.P., "ASTOVL Model Engine Simulators for Wind Tunnel Research", Paper 15, AGARD CP-498 (October 1991).

3. LAUGHREY, J.A. & MOORHOUSE, D.J., "Propulsion Integration Results of the STOL Manoeuvre Technology Demonstrator", Paper 30, AGARD CP-498, (October 1991).

4. ANON, "EN COUVERTURE", Air & Cosmos / Aviation International No. 1439, 20-26 Sept.1993.

5. ALLEN, D.A., SLEEMAN, J.R. & WELLER, B.R.C., "The Integrated Flight & Powerplant Control System Demonstration Programme", AIAA 93-4830, 1993.

7. FRANKLIN, J.A., Experience with Integrated Flight/Propulsion Controls from Simulation of STOVL Fighter Concepts", AIAA 93-4874, 1993.

8. WARDWELL, D.A. & HANGE, C.E., "Jet-Induced Lift Characteristics of a 5.3% Scale Model of the Mixed-Flow Vectored-Thrust (MFVT) ASTOVL Concept", AIAA 93-4817, 1993.

9. NANGIA, R.K., "Vectored Jets-Induced Interference on Aircraft, Prediction & Verification", AGARD FDP 72nd Meeting, Winchester, April'93.

10. NANGIA, R.K., "Estimating Wind Tunnel Interference Due To Vectored Jet Flows", AGARD FDP 73rd Meeting, Brussels, October'93.

11. JORDINSON, R., "Flow in a Jet Directed Normal to the Wind", A.R.C. R & M 3074, 1958.

12. THOMPSON, A.M. " The Flow induced by Jets Exhausting Normally from a Plane Wall into an Airstream", PhD Thesis, Uni. of London, 1971.

13. FEARN, R.L. & WESTON, R.P., "Vorticity Associated with a Jet in a Crossflow", AIAA J. of Air., Vol.12, No.12, pp.1666-71, (Dec.1974).

14. FEARN, R.L. & WESTON, R.P., "Induced Velocity Field of a Jet in a Crossflow", NASA TP-1087, (1978).

15. FEARN, R.L. & WESTON, R.P., "Velocity Field of a Round Jet in a Crossflow for Various Jet Injection Angles and Velocity Ratio", NASA TP-1506, (1979).

16. FEARN, R.L., "Velocity Field of a Round Jet in a Crossflow for Various Jet Injection Angles and Velocity Ratio", Proceedings of Conference held at University of Stanford in 1983, Published in "Recent Advances in Aerodynamics", Springer Verlaag, 1986.

17. TOY, N. & SAVORY, E., "An Experimental Study of a Jet in Cross-flow", Surrey University, Guildford, Dec.1988.

18. BRADBURY, L.J.S., "Some Aspects of Jet Dynamics and their Implications for VTOL Research", AGARD-CP-308, (1981).

19. SMY, J.R. & RANSOM, E.C.P., "Structure of Single Jets at Large Angles to Cross-Flow", BAe Kingston Internal Report, (1976).

20. WOOLER, P.T., KAO, H.C., SCHWENDAM, M.F. & ZIEGLER, H., "VSTOL Aircraft Aerodynamic Prediction Methods", AFFDL-TR-72-26, (1972).

21. HACKETT, J.E., "Living with Solid-Walled Wind Tunnels", AIAA-82-0583, 1982.

22. ASHILL, P.R. & KEATING, R.F.A., "Calculation of Tunnel Wall Interference from Wall-Pressure Measurements", Euromech Colloquium 187, Oct.1984, DFVLR, Gottingen, (See also RAE TR 85086, (1985).

23. MARGASON, R., "Fifty Years of Jet in Cross-flow Research", AGARD FDP 72nd Symposium, Winchester UK, April 1993.

24. KUHN, R.E., "The Induced Aerodynamics of Jet and Fan Powered V/STOL Aircraft", Proc. of Intern. Symposium, Stanford, Aug. 1983, "Recent Advances in Aerodynamics", Editors: KROTHPALLI, A. & SMITH, C.W., Springer-Verlag (1986).

25. KOTANSKY, D.R., "Jet Flowfields", AGARD Report 710, 1984.

26. HANCOCK,G.J.,"A Review of the Aerodynamics of a Jet in a Cross Flow", The RAeS Aeronautical Journal, Vol.91., No.905, pp. 201-13, May 1987.

27. CHIU, S., ROTH, K.R., MARGASON, R.J. & TSO, J., "A Numerical Investigation of a Subsonic Jet in a Crossflow", AIAA 93-0870 (1993).

28. ANDERSON, J.D., "Fundamentals of Aerodynamics", McGraw Hill, 1984.

29. DENNIS, R.F., TSO, J. & MARGASON, R.J., "Induced Surface Pressure Distribution of a Subsonic Jet in a Cross-Flow", AIAA-93-4861, 1993.

30. GIESING, J.P., KALMAN, T.P. & RODDEN, W.P., "Subsonic Steady and Oscillatory Aerodynamics for Multiple Interfering Wings and Bodies", J. of Air., Vol.9, No. 10, pp. 693-703, October 1972.

31. Airplane Part 6, Published by Orbis.

LIST OF SYMBOLS

A = ¼ π D^2, Nozzle cross-section Area
CG Centre of Gravity
C_{LL} Local Lift Coefficient
C_P Pressure Coefficient
C_μ = T/(q S), Thrust Force Coefficient
D Jet Nozzle Diameter
F Scaling Factor, Jet vortex path in free air
L Lift Force
LE Leading Edge
q = 0.5 ρ V^2, Dynamic Pressure
R = V_j/V, Jet Velocity Ratio
s Wing Semi-Span
S Wing Reference Area
T or μ Jet Thrust
TE Trailing Edge
u,v,w perturbation or induced velocities in x,y,z direction
V Airstream Velocity
V_j Nozzle Jet Velocity
x,y,z Orthogonal Co-ordinates, x chordwise
z_j Distance along z measured from jet nozzle face
z_w Distance along z measured from jet nozzle face to wing surface
α Angle of attack
μ_T Doublet Strength
σ_v source strength along jet
σ_{v0} source strength at jet origin
Θ_{j0} Nozzle Jet Deflection angle with respect to free-stream
Θ_j Jet vortex path Deflection angle with respect to free-stream
ρ Air Density